FORWARD–BACKWARD MULTIPLICITY CORRELATIONS IN RELATIVISTIC HEAVY-ION COLLISIONS

Waseem Bari, Qudsia Gani, Shamsul H. Thoker
Muzamil A. Teli

Department of Physics, University of Kashmir, Srinagar — 190 006, India

(Received July 28, 2014; revised version received April 16, 2015)

This study presents the investigations on the occurrence of multiplicity correlations in the particle multiplicities in forward and backward hemisphere in the multiparticle states produced in ^{28}Si nuclei with various targets at two different energies. The forward–forward and forward–backward dispersions are looked into. The variation of the correlation strength as a function of the pseudorapidity range is investigated and its dependence on target mass as well as the incident energy is studied. In order to estimate the contribution of non-statistical fluctuations, we use the deviation of the value of effective cluster multiplicity from unity as the benchmark.

DOI:10.5506/APhysPolB.46.2039
PACS numbers: 25.75.–q, 25.75.Gz, 25.75.Nq, 12.38.Mh

1. Introduction

One of the major goals of studying heavy-ion collisions at relativistic energies is to have a better understanding of the formation and evolution of the QCD matter [1] in such collisions. This is because the quantum chromodynamics (QCD) predicts that in relativistic heavy-ion collisions, the conditions of sufficiently high energy density, of the order of 0.5 GeV/fm^3 [2], which is necessary to establish the presence of a deconfined phase of quarks and gluons are produced. Most of the heavy-ion programs around the world are being executed with a special focus on disentangling the information about this particular phase of matter which is referred to as the quark–gluon plasma (QGP). In the most recent past, experimental studies at the RHIC [3] and LHC [4] have had convincing evidence in support of the formation of a deconfined phase of quarks and gluons. Although the theoretical physics community has proposed a great deal of insight into the possible occurrence of the deconfined phase [5], for an experimentalist, it is also important to have an understanding of the observables which could actually be tested on a theoretical model to establish the physical phenomena taking place during the process and to have an understanding of the evolution of the processes. One such approach is to investigate the correlations amongst the particles emitted at the freeze-out of QGP which could actually shed light on the earlier stages of the heavy-ion collisions too. Most recently, the correlations have beeen studied in proton–nucleus and nucleus–nucleus collisions at the LHC and RHIC [6, 7].

In the present work, we are investigating the forward–backward (FB) correlations of charged particle yields (the multiplicity correlations) in nucleus–nucleus collisions at 4.5 A and 14.5 $A\,\mathrm{GeV}/c$ energies.

The paper is organized as follows. In Section 2, we briefly discuss the importance of studying the forward–backward correlations in the multiplicities of the final state particles produced in relativistic heavy-ion collisions. In Section 3, the method of analysis and the various observables have been defined. Section 4 exhibits the details of the experimental data which have been used for the analysis in the present study. In Section 5, we discuss the results on these observables and the various analyses carried out. Finally, in Section 6, a brief summary of the findings is presented.

2. Forward–backward correlations

The investigation of forward–backward (FB) correlations between various observables is considered to be a powerful tool for defining the initial conditions for the formations of QGP [8, 9]. These types of correlations could have components coming from both short-range as well as long-range correlations. The short-range correlation component arises from narrow pseudorapidity regions whereas the long-range components originate from the extended pseudorapidity interval [10]. Investigation of FB multiplicity correlations have been carried out in the past over a wide range of energies and for a wide spectrum of projectile–target combinations [11–15]. Recently, NA22 Collaboration [16] investigated in detail the correlations in nucleus–nucleus collisions. Most recent studies on this very important aspect have been based on the data from the STAR experiment at RHIC [17, 18] and ALICE experiment at the LHC [10].

The importance of studying FB correlations is multi-dimensional. One of the motivation comes from the realization that during a nucleus–nucleus collision, quark–gluon strings originating from hadron–hadron collision and stretched in rapidity may be formed [19]. These strings in the environment of high energy density could interact [20] resulting in the string fusion leading to the formation of QGP. Several studies [21] indicated that the study of forward–backward correlations of particles produced in heavy-ion collisions at high energies could be a strong tool to have a more clear understanding of the processes of the string fusion, the cluster formation and other decay processes. The long-range correlations between various observables, measured in sufficiently separated rapidity intervals, may appear as the signal relevant to string fusion, while a decay of clusters of particles and resonances is marked by increased short-range correlations [10]. The formation of Colour Glass Condensates (CGC) [22] is yet another field which has been proposed [23] to be studied with the help of the multiplicity correlation strength in relativistic heavy-ion collisions. Therefore, the detailed experimental studies of the correlation strength and its rapidity structure are crucial for understanding of the physics of the hadron–nucleus and nucleus–nucleus collision process, in general.

3. Method of analysis

First of all, the whole pseudorapidity space in the center-of-mass coordinate system is divided into the forward and backward hemispheres which lie conventionally opposite to each other on the basis of the two opposite sides of a reference value of pseudorapidity, which in our case is η_0. The forward and backward hemispheres in the present context can be realized by the schematic representation of the regions shown in Fig. 1. N_f and N_b

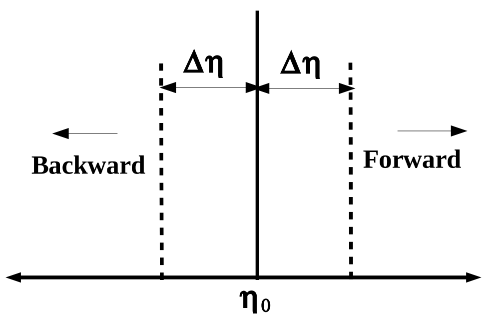

Fig. 1. Definition of forward and backward hemispheres.

are the charged particle multiplicities within the forward and backward intervals within a width of $\Delta\eta$ on the two sides of η_0. In our analysis, we have measured the correlations amongst the particles with varying $\Delta\eta$ values on both the sides. The parameter which is used to characterize FB correlations is the correlation strength, b_corr which is extracted from the slope of a linear relationship between the average multiplicity measured in the backward rapidity hemisphere, N_b, and the multiplicity in the forward rapidity hemisphere, N_f. This relationship is expressed as [24]

$$\langle N_\mathrm{b}\left(N_\mathrm{f}\right)\rangle = a + b_\mathrm{corr} N_\mathrm{f}\,. \tag{1}$$

The correlation coefficient can be positive or negative within a range of $|b_{\rm corr}| < 1$. The extreme values of -1 and $+1$, respectively, represent the total correlation and total anti-correlation of the produced particles separated in rapidity. The value $b_{\rm corr} = 0$ is the limiting case of entirely uncorrelated particle production. The intercept, a, is related to the uncorrelated particle number in the collision. The correlation coefficient is also expressible in terms of the covariance of forward–backward multiplicity and the variance of the forward multiplicity. This form is obtained by performing a linear regression of Eq. (1) and minimizing the χ^2 so that the correlation coefficient attains the following form

$$b_{\rm corr} = \frac{\langle N_{\rm f} N_{\rm b}\rangle - \langle N_{\rm f}\rangle \langle N_{\rm b}\rangle}{\left\langle N_{\rm f}^2\right\rangle - \langle N_{\rm f}\rangle^2} = \frac{D_{\rm bf}^2}{D_{\rm ff}^2}\,. \tag{2}$$

$D_{\rm fb}^2 = \langle N_{\rm f} N_{\rm b}\rangle - \langle N_{\rm f}\rangle \langle N_{\rm b}\rangle$ and $D_{\rm ff}^2 = \left\langle N_{\rm f}^2\right\rangle - \langle N_{\rm f}\rangle^2$, respectively, represent the forward–backward and forward–forward dispersions.

As stated earlier, the correlations could be having both short-range, those pertaining to a narrow pseudorapidity window, as well as the long-range component, those coming from wider pseudorapidities window. In the present work, we have chosen the range which would actually cover the whole experimental observation range. The individual contributions would be investigated and discussed in Section 5.

It has been proposed [25, 26] that the FB correlations could be investigated by comparing the charged particle multiplicities in forward (F) and backward (B) hemispheres which are defined as the regions on the opposite sides of the centre-of-mass rapidity $\eta_{\rm c}$, *i.e.*, the forward regions correspond to $\eta > \eta_{\rm c}$, where as $\eta < \eta_{\rm c}$ represents the backward hemisphere. The behaviour of the variation of the charged particles produced in the two regions is represented on an event-by-event basis by the asymmetry parameter, C, defined as [27, 28]

$$C = \frac{N_{\rm f} - N_{\rm b}}{\sqrt{N_{\rm f} + N_{\rm b}}}\,. \tag{3}$$

This parameter is useful in discriminating between the different kinematical regions within a pseudorapidity space as it has been suggested [28] that for bins covering similar kinematical regions, the asymmetry parameter should tend to have a value very close to zero.

The variance of the asymmetry parameter is given by

$$\sigma_C^2 = \frac{D_{\rm ff}^2 + D_{\rm bb}^2 - 2D_{\rm fb}^2}{\langle N_{\rm f} + N_{\rm b}\rangle}\,, \tag{4}$$

where $D_{\rm bb} = \left\langle N_{\rm b}^2\right\rangle - \langle N_{\rm b}\rangle^2$ represents the variance of the backward hemisphere. The angular brackets refer to the fact that the quantities have been averaged over the whole event sample. The behaviour of this parameter is usually used to investigate the presence/absence of non-statistical fluctuations in the multiparticle production in relativistic heavy-ion collisions. If the value of the variance is close to unity, *i.e.*, $\sigma_C^2 \approx 1$, this would actually refer to the absence of any dynamical fluctuations whereas a deviation from the unit value would be an indication of the presence of non-statistical fluctuations in the multiparticle production [27, 28].

4. Details of the data

For the present investigations, a random sample of 555 interaction events occurring in the interactions of ^{28}Si nuclei with emulsion at 4.5 A GeV energy have been analyzed. These events have been taken from the emulsion stacks exposed to 4.5 A GeV/c silicon beam from Synchophasotron at Dubna. We have selected the events with $n_{\rm s} \geq 2$, where $n_{\rm s}$ represents the number of charged particles produced in an event with relative velocities $\beta \geq 0.7$. The emission angles of all the relativistic charged particles were measured and their pseudorapidities were determined. All other relevant details about the stacks used, criteria employed for selecting the events and the method of measuring the emission angles may be found elsewhere [29, 30] and the references therein. For comparing the results with incident energy, a sample of 530 interactions of the same criteria obtained from the exposure of emulsion stacks to 14.5 A GeV/c silicon beam from AGS at BNL have been used.

5. Results and discussion

The results on the variances, covariance, correlation coefficient and the variance of the asymmetry parameter are discussed in the following subsections.

5.1. Dispersions

In the present work, the FB correlations have been studied for the interactions of ^{28}Si with various targets at two different energies, *i.e.*, 4.5 A and 14.5 A GeV/c. The forward–forward and forward–backward dispersions have been calculated within a pseudorapidity gap extending up to 3.25 units on both sides of the central value of the pseudorapidity which, in the present case, is taken to be zero. The variations of the dispersions with the pseudorapidity gap are exhibited in Fig. 2. One important observation which comes to light is that the forward–forward dispersions are higher than those of forward–backward dispersions. The difference is more prominent when the energy increases. Further, it is observed that the prominence in the difference between the two dispersions increases as the pseudorapidity gap considered increases. It is also worth noticing that the trends seen in the plots indicate an almost constant dispersion (forward–forward as well as forward–backward) after a certain value of the pseudorapidity window, with this limit reaching more quickly and more prominently at higher energy.

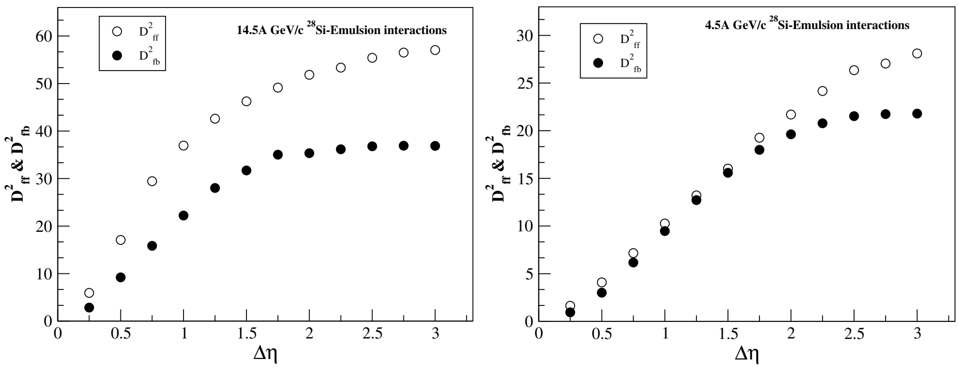

Fig. 2. Variation of the dispersions at two energies.

In Fig. 3, we present the results on forward–forward dispersion as a function of the pseudorapidity window used at the two energies for different targets in order to investigate if there exists any dependence of the variation on the target size. It is seen that the dispersions are higher for heavier targets at both the energies. However, one can observe that for higher energy, the dispersions differ more at larger pseudorapidity windows whereas at lower energy, the dispersions differ less at higher pseudorapidity window. This might be an indication of the presence of long-range correlations amongst the particles produced at higher energies and, at the same time, the presence of short-range correlations at lower energies.

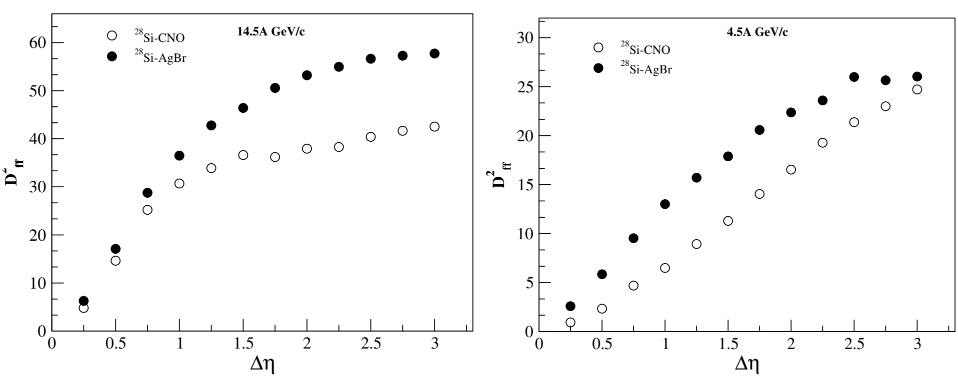

Fig. 3. Target dependence of the forward–forward dispersions at two energies.

In order to look for any target dependence of the forward–backward dispersions, the variations of the same width $\Delta\eta$ for different targets at the two energies are exhibited in Fig. 4. There are two important observations from the trends exhibited by the forward–backward dispersion. Firstly, it is observed that the dispersions are higher for heavier targets, although the difference becomes more prominent at larger pseudorapidity windows. Secondly, the dispersions tend to saturate at higher $\Delta\eta$ values. The first observation may be an indication of the fact that with the increase in the target size, we have more relativistic charged particles which normally lie in the forward cone of the pseudorapidity space.

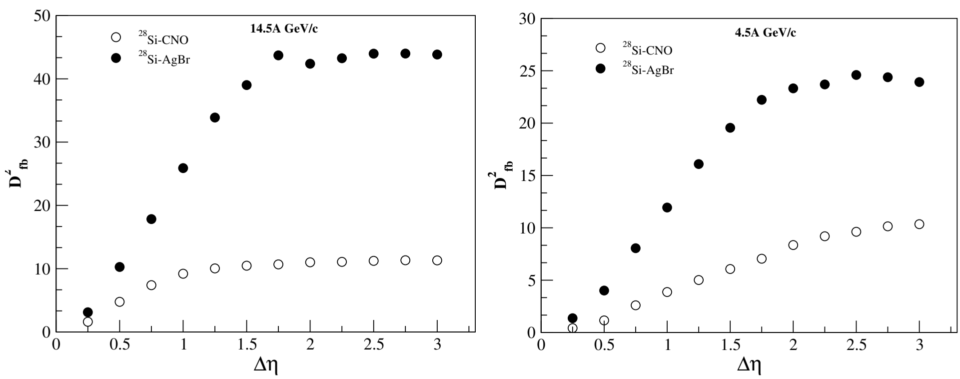

Fig. 4. Target dependence of the forward–backward dispersions at two energies.

5.2. Correlation coefficient

Results on the variation of the correlation strength are presented in Figs. 5 and 6. In Fig. 5, the variation of the correlation coefficient with $\Delta\eta$ is shown for the ^{28}Si–emulsion interactions at 4.5 A and 14.5 $A\,\mathrm{GeV}/c$. It is observed that the correlation coefficient exhibits a similar trend with the pseudorapidity interval at both the energies. However, within a particular pseudorapidity range, the correlation amongst the secondary particles seems to be stronger at lower energy. One more observation from this figure is that the correlation becomes stronger at around $\Delta\eta = 1.5$. This might be a reflection of the fact that for the pseudorapidity range considered in the present study, this value represents the central region on both sides of the reference value. As such, it is expected that strongest correlation would exist there. In order to understand if the target size plays a role in the correlation strength, we have plotted the correlation coefficient for two different targets at both the energies in Fig. 6. We observe that in the case of heavier target, the correlation coefficient has a larger value. However, for both the targets, it seems that the correlation strength tends to saturate after a certain pseudorapidity value which, in our case, may be attributed to lower statistics of particles in that region.

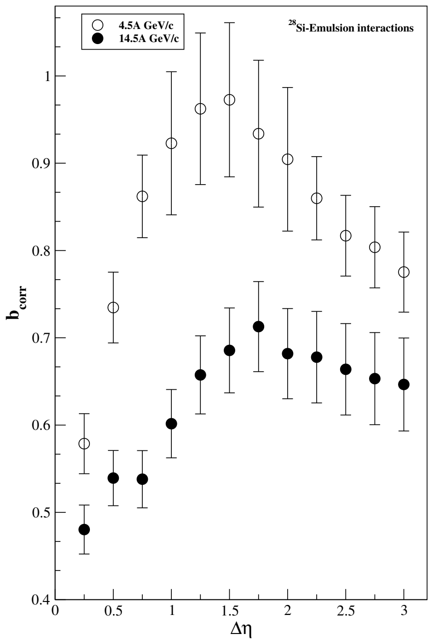

Fig. 5. Variation of the correlation coefficient at two energies.

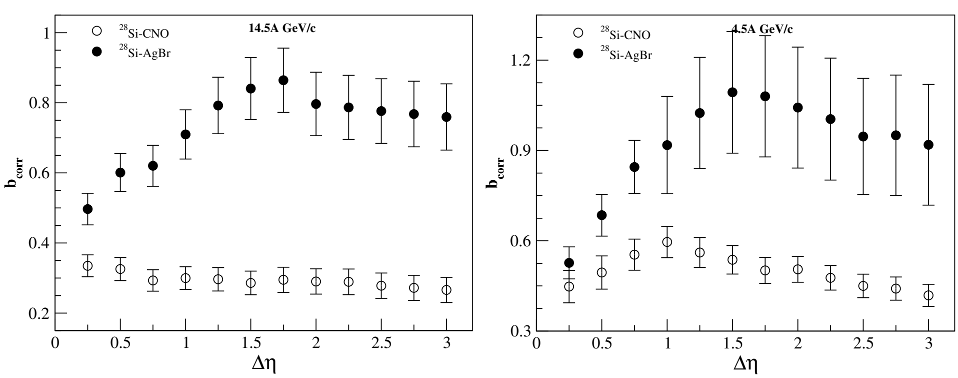

Fig. 6. Variation of the correlation coefficient at two energies for different targets.

5.3. Effective cluster multiplicity

The asymmetry parameter, C, defined by Eq. (3) is insensitive to the dependence of multiplicity on centrality of the collision [31]. It has been proposed that the variance defined above by Eq. (4) measures the strength of multiplicity fluctuations. If the fluctuations have purely statistical origin, then $\sigma_C^2 = 1$ whereas a deviation from this value would be suggestive of the dynamical origin of these fluctuations. The variations of σ_C^2 with the pseudorapidity bin $\Delta\eta$ for ^{28}Si–emulsion interactions at 4.5 A and 14.5 $A\,\mathrm{GeV}/c$ are plotted in Fig. 6. It is observed that with the increase in $\Delta\eta$, the value of σ_C^2 increases and so does its deviation from unity. This behaviour is in agreement with what has been observed earlier [32] and explained on the basis of cluster model. In Fig. 7, we also observe that at higher incident energies, the deviations of σ_C^2 from unity are higher, thereby indicating that the multiplicity fluctuations at higher energies may have more dynamical origin than at lower energies.

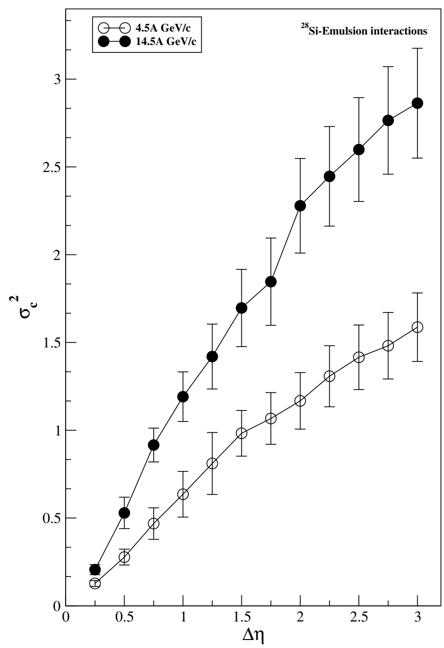

Fig. 7. Variation of σ_C^2 with the pseudorapidity window for ^{28}Si–emulsion interactions at 4.5 A and 14.5 $A\,\mathrm{GeV}/c$.

In order to investigate whether there is any role of target size in the presence of non-statistical fluctuations, the variations of σ_C^2 with the pseudorapidity bin $\Delta\eta$ for ^{28}Si nuclei with CNO and AgBr targets are plotted in Fig. 8. It is observed that at 4.5 $A\,\mathrm{GeV}/c$, the values of σ_C^2 are higher in the case of interactions with AgBr than those in the case of interactions with CNO in the whole range of pseudorapidity investigated in the present study which indicates that interactions due to heavier target have more contribution to the multiplicity fluctuations than those due to lighter target. However, when the incident energy increases almost threefold, it is observed that in a narrower pseudorapidity bin, $\Delta\eta$, the lighter target has more contribution. When the range is widened, the deviation of the variance in the asymmetry parameter is higher in the case of heavier target. This may be due to the presence of large fluctuations in the pseudorapidity region which is away from the centre-of-mass rapidity region.

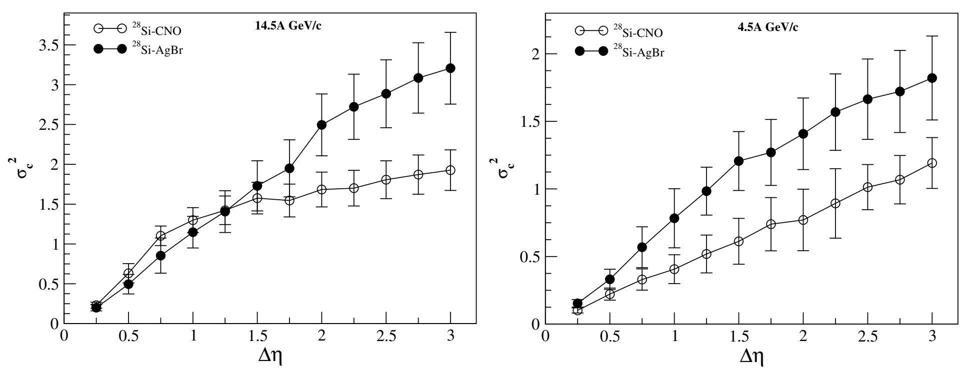

Fig. 8. Variation of σ_C^2 with the pseudorapidity window for the interactions of ^{28}Si nuclei with CNO and AgBr targets at 4.5 A and 14.5 $A\,\mathrm{GeV}/c$.

6. Summary

The forward–backward multiplicity correlations amongst the relativistic charged particles produced in the interactions of ^{28}Si nuclei with various targets at 4.5 A and 14.5 $A\,\mathrm{GeV}/c$ are investigated. It is found that the forward–forward as well as forward–backward dispersions show an increasing trend with increasing pseudorapidity range at both the energies. The dispersions show a saturating behaviour with wider pseudorapidity which is more prominent at higher energy. The dispersions show a similar trend at all the targets chosen. However, it is observed that for the interactions due to heavier target, the dispersions have higher values than the dispersions in the case of interactions due to lighter targets.

On comparison of the strength of the correlation at two different energies, it is found that the correlation coefficient has a higher value at higher energy. Further, the comparison of the correlation coefficient for different targets reveals that for the interactions due to heavier targets, the correlations amongst the relativistic charged particles seems to be higher. The presence of the non-statistical contribution to the fluctuations in the multiparticle final state is looked into in terms of the deviation of the effective cluster multiplicity σ_C^2 from unity. The behaviour exhibited by this parameter in our study is well in agreement with what has been suggested on the basis of the cluster model.

One of us (W.B.) acknowledges the help of Dr. Manzoor A. Malik, presently the Head of the Department of Physics, support and fruitful discussions.

REFERENCES

[1] H. Satz, *Rep. Prog. Phys.* **63**, 1511 (2000); S.A. Bass, M. Gyulassy, H. Stöcker, W. Greiner, *J. Phys. G* **25**, R1 (1999); E.V. Shuryak, *Phys. Rep.* **115**, 151 (1984); J. Cleymans, R.V. Gavai, E. Suhonen, *Phys. Rep.* **130**, 217 (1986).

[2] S. Borsanyi *et al.*, *J. High Energy Phys.* **1011**, 77 (2010).

[3] I. Arsene *et al.* [BRAHMS Collaboration], *Nucl. Phys. A* **757**, 1 (2005); K. Adcox *et al.* [PHENIX Collaboration], *Nucl. Phys. A* **757**, 184 (2005); B.B. Back *et al.* [PHOBOS Collaboration], *Nucl. Phys. A* **757**, 28 (2005); J. Adams *et al.* [STAR Collaboration], *Nucl. Phys. A* **757**, 102 (2005).

[4] K. Aamodt *et al.* [ALICE Collaboration], *Phys. Rev. Lett.* **105**, 252302 (2010); *Phys. Rev. Lett.* **107**, 032301 (2011); G. Aad *et al.* [ATLAS Collaboration], *Phys. Rev. Lett.* **105**, 252303 (2010); K. Aamodt *et al.* [ALICE Collaboration], *Phys. Lett. B* **696**, 30 (2011).

[5] P. Steinberg [ATLAS Collaboration], *Nucl. Phys. A* **932**, 9 (2014); B. Mueller, Proceedings of KMI-GCOE Workshop Nagoya University, Nagoya, Japan, December 4–7, 2012; H. Satz, *Phys. Rep.* **403–404**, 33 (2004); *J. Phys. G* **32**, R25 (2006); K. Fukushima, T. Hatsuda, *Rep. Prog. Phys.* **74**, 014001 (2011).

[6] K. Aamodt *et al.*, *Phys. Lett. B* **708**, 249 (2012).

[7] B. Abelev *et al.*, *Phys. Lett. B* **719**, 29 (2013).

[8] A. Dumitru *et al.*, *Nucl. Phys. A* **810**, 91 (2008).

[9] N. Armesto, L. McLerran, C. Pajares, *Nucl. Phys. A* **781**, 201 (2007).

[10] G.A. Feofilov *et al.*, XXI International Baldin Seminar on High Energy Physics Problems, JINR, Dubna, Russia, 2012.

[11] W. Braunschweig *et al.* [TASSO Collaboration], *Z. Phys. C* **45**, (1989).

[12] P. Abreu *et al.* [DELPHI Collaboration], *Z. Phys. C* **50**, 185 (1991).

[13] R. Akers, *Phys. Lett. B* **320**, 417 (1994).

[14] V.V. Aivazyan *et al.* [NA22 Collaboration], *Z. Phys. C* **42**, 533 (1989).

[15] T. Alexopoulos *et al.*, *Phys. Lett. B* **353**, 155 (1995).

[16] G.A. Feofilov *et al.* [NA49 Collaboration] "Long-Range Correlations in Pb–Pb Collisions at 158 A GeV", Proc. XVII ISHEPP, JINR, Dubna vol. 1, 2005, p. 222.

[17] B.I. Abelev [STAR Collaboration], *Phys. Rev. Lett.* **103**, 172301 (2009) [`arXiv:0905.0237 [nucl-ex]`].

[18] Quan Wang, Fuqiang Wang, *MNRAS* **419**, 1610 (2012) [`arXiv:1109.3157 [astro-ph.SR]`].

[19] A. Capella, U.P. Sukhatme, C.I. Tan, J. Tran Thanh Van, *Phys. Lett. B* **81**, 68 (1979); *Phys. Rep.* **236**, 225 (1994); A.B. Kaidalov, K.A. Ter-Martirosyan, *Phys. Lett. B* **117**, 247 (1982).

[20] V.A. Abramovskii, E.V. Gedalin, E.G. Gurvich, O.V. Kancheli, *JETP Lett.* **47**, 337 (1988).

[21] N.S. Amelin *et al.*, *Phys. Rev. Lett.* **73**, 2813 (1994).

[22] L. McLerran, *Nucl. Phys. A* **699**, 73 (2002).

[23] T. Lappi, L. McLerran, *Nucl. Phys. A* **832**, 330 (2010) [`arXiv:0909.0428 [hep-ph]`].

[24] G.J. Alner *et al.*, *Phys. Rep.* **154**, 247 (1987).

[25] K. Wozniak [PHOBOS Collaboration], *Int. J. Mod. Phys. E* **16**, 2187 (2007).

[26] P. Steinberg *et al.* [PHOBOS Collaboration], *Nucl. Phys. A* **774**, 631 (2006).

[27] S. Haussler *et al.*, *Nucl. Phys. A* **785**, 253 (2007).

[28] K. Wozniak [PHOBOS Collaboration], `arXiv:1005.1478 [nucl-ex]`.

[29] A. Shakeel *et al.*, *Int. J. Mod. Phys. E* **18**, 131 (1999).

[30] W. Bari *et al.*, *Int. J. Mod. Phys. E* **11**, 131 (2002).

[31] K. Wozniak [PHOBOS Collaboration], `arXiv:1005.1478 [nucl-ex]`.

[32] A. Shakeel *et al.*, *Phys. Scr.* **87**, 045201 (2013).